J. Fluid Mech. (1988), *vol.* 195, *pp.* 523–540
Printed in Great Britain

Buckling instabilities in layers of viscous liquid subjected to shearing

By T. BROOKE BENJAMIN AND T. MULLIN
Mathematical Institute, 24/29 St Giles, Oxford OX1 3LB, UK

(Received 11 December 1987)

A theoretical and experimental investigation is reported dealing with the onset of buckling in a horizontal layer of highly viscous liquid. The layer floats on a heavier liquid with negligible viscosity, and at rest is stabilized by gravity and surface tension. When sheared at a sufficient rate, the flat configuration of the layer becomes unstable; and the aim of the investigation is to establish the relation between critical values of the shearing rate and values of the layer's thickness and other physical parameters.

A primitive theory based on membrane approximations is first reviewed and its deficiencies are appreciated. Then a more reliable theory is developed, providing estimates of values taken by a dimensionless shear stress f at the threshold of instability. The values f_c are found to depend primarily on a dimensionless number H proportional to the thickness of the layer.

Experiments on sheared layers of silicone oil with various high viscosities are then described. Measured values of f_c plotted against H over a wide range are shown to be in satisfactory agreement with the theory. Finally, discrepancies between previous experimental results and ours are discussed.

1. Introduction

Layers of highly viscous liquid are well known to develop buckling instabilities when compressed or sheared in their plane at sufficient rates. This paper presents a theoretical and experimental examination of conditions for the onset of buckling in a horizontal layer of viscous liquid subject to pure shearing, whose destabilizing effect is opposed by gravity and surface tension. The agreement established between theory and experiment is more satisfactory than achieved in previous investigations, notably that by Suleiman & Munson (1981).

Most inquiries into this subject over recent years have acknowledged the stimulus of a short article by Taylor (1969) which reported various experiments, although earlier antecedents include theoretical studies by Ramberg (1963), Biot (1964) and others which were directed towards geophysical applications. It will be of particular interest at present to recall one of Taylor's demonstrations (1969, figures 15–17) in which a distinctive form of buckling appeared as an instability phenomenon in a sheared annular layer of viscous liquid (golden syrup with a viscosity of about 40 P). A simple theoretical interpretation based on membrane approximations was cited by Taylor, and it appeared to account for certain of his observations. The simple theory is defective, however, and in §2 it will be outlined in order to prepare the way for a more reliable theory presented in §3. Incidentally, at the end of §2, the likely explanation for Taylor's observations will be noted, in support of which some experiments made soon after and matching his will be reported for the first time.

Since Taylor's focal contribution, viscous buckling under compression has been studied theoretically by several authors, among whom Buckmaster & Nachman (1978) included surface tension in their model and Wollkind & Alexander (1982) allowed for both surface tension and gravity in theirs. Although primarily intended to illuminate the geological phenomenon of rock-folding, the theoretical work by the latter authors came closest in substance to our theory in §3. Because of various differences in formulation, their results are not adaptable securely to the present problem. It is notable, however, that they were the first to demonstrate an optimal dimensionless thickness, at which the dimensionless loading sufficient to buckle a viscous layer is an absolute minimum (1982, Fig. 5). A comparable property will be found in §3 and borne out by our experimental findings presented in §5.

Suleiman & Munson (1981) have reported extensive experiments with an apparatus that was the same in principle as Taylor's and ours. They studied a variety of highly viscous liquids floated on various heavier, comparatively inviscid liquids, and they tried a moderately wide range of layer thicknesses. They also measured the relation between angular speed of the rotated boundary and torque exerted on the opposite boundary, using the change in the slope of this relation as an indicator of incipient buckling. The simple theory suggested by Taylor (1969) was cited by them in a brief theoretical appraisal, but they acknowledged its failure to explain their experimental observations. In particular, they noted that measured critical values of the shear stress τ could be correlated well by the dimensionless ratio $\tau/(g\rho_2 T)^{\frac{1}{2}}$, where ρ_2 is the density of the supporting liquid and T the net surface tension, this correlation being conspicuously better than by τ(layer thickness)/T as indicated by the simple theory.

In §3.4, confirming Suleiman & Munson's empirical discovery, the dimensionless shear stress $f = \tau/(g\rho_2 T)^{\frac{1}{2}}$ will be shown theoretically to be the decisive parameter for buckling. Critical values f_c of f will be calculated as a function of the dimensionless ratio $H = 2h(g\rho_2/T)^{\frac{1}{2}}$, where $2h$ is the thickness of the sheared layer. Our experimental results reported in §5 agree closely with the predicted relation of f_c to H, but a particularly sensitive method for the detection of incipient buckling was needed to establish the agreement. Our measurements of f_c do not agree with Suleiman & Munson's, however, being typically 50% of theirs. The discrepancy will be discussed in §6.

2. Theory based on membrane approximations

The simple theory cited by Taylor (1969) and Suleiman & Munson (1981) deserves to be summarized, for it exposes requirements to be met by the more accurate theory that will be presented in §3. As far as we are aware, an explicit account of the simple theory has not been given before, and its apparent success in explaining Taylor's experimental observations has yet to be explained properly.

The model in question can be appreciated as an immediate adaptation of well-known results for thin elastic plates perturbed from a planar state (see Timoshenko 1940, §58). For a plate of uniform thickness $2h$ composed of elastic material with Young's modulus E and Poisson's ratio ν, the bending stiffness (flexural rigidity) is given by $B = 2Eh^3/3(1-\nu^2)$ (Timoshenko 1940, p. 3). If the material is incompressible, one has $\nu = \frac{1}{2}$ and $E = 3G$, where G is the modulus of rigidity; hence $B = (\frac{8}{3})Gh^3$. This result shows at once how the equation expressing the equilibrium of an infinitesimally perturbed elastic plate (Timoshenko 1940, p. 301) is adaptable to the case of a thin layer composed of incompressible liquid with viscosity μ.

Because the supporting analysis is precisely analogous, the only change is that B in the original equation is replaced by the operation $b\partial/\partial t$ with

$$b = \tfrac{8}{3}\mu h^3. \tag{1}$$

Thus, taking Cartesian coordinates (x, y) in the plane of the unperturbed layer, writing $\xi(x, y, t)$ for its infinitesimal displacement perpendicular to this plane, and supposing the layer to support direct-stress resultants N_x, N_y, a shear-stress resultant N_{xy} (i.e. net forces per unit span in the plane of the unperturbed layer) and a lateral external load q per unit area, we infer the equation

$$b\Delta^2\left(\frac{\partial \xi}{\partial t}\right) = N_x \frac{\partial^2 \xi}{\partial x^2} + N_y \frac{\partial^2 \xi}{\partial y^2} + 2N_{xy}\frac{\partial^2 \xi}{\partial x\, \partial y} + q \tag{2}$$

(cf. Timoshenko 1940, p. 301, equation (175)). Here Δ denotes the Laplacian operator $\partial_x^2 + \partial_y^2$.

Let us assume the layer to suffer no compression nor stretching, so that N_x and N_y both reduce to a positive constant T which is the sum of the surface tensions on the upper and lower surfaces of the layer. The layer is taken to undergo shearing in its plane, however, say at a rate $S = S(x, y)$; and so the shear stress μS acting over the thickness $2h$ amounts to $N_{xy} = 2\mu Sh$. Next, assuming the layer of viscous liquid with density ρ_1 to float on a liquid with density $\rho_2 > \rho_1$ and negligible viscosity, we deduce that $q = -g\rho_2 \xi$. (This conclusion recognizes that the effects of gravity on flexural deformations of the layer appear only through the hydrostatic variation of pressure on the lower side of the interface between the two liquids; for, according to the approximations implicit in (2), the thickness of the layer is invariant.) Thus (2) becomes

$$b\Delta^2\left(\frac{\partial \xi}{\partial t}\right) = 4\mu Sh \frac{\partial^2 \xi}{\partial x\, \partial y} + T\Delta\xi - g\rho_2\, \xi, \tag{3}$$

which linear partial differential equation for ξ is the crux of the simple theory.

A local criterion of stability can be deduced plausibly from (3) as follows, without reference to boundary and initial conditions which would be needed for a complete description of possible motions. Taking α and β to be real numbers, consider

$$\xi' = a(t) \cos(\alpha x - \beta y + \text{const.}) \tag{4}$$

as the generic Fourier component in a representation of ξ valid over a region of the (x, y)-plane wherein S is approximately constant. Write $k = (\alpha^2 + \beta^2)^{\frac{1}{2}} > 0$ and $\theta = \arctan(\beta/\alpha)$. Then substitution of (4) into (3) gives at once

$$\frac{1}{a}\frac{\mathrm{d}a}{\mathrm{d}t} = \frac{(2\mu Sh \sin 2\theta - T)\, k^2 - g\rho_2}{bk^4}. \tag{5}$$

Buckling instability is indicated by exponential growth of the amplitude a, as occurs when the right side of (5) is positive for some real values of k and θ. If $S > 0$, maximum growth evidently requires $\sin 2\theta = 1$: that is, $\theta = \frac{1}{4}\pi$ or $\beta = \alpha$, and the waveform (4) then has its lines of constant phase at 45° to the x-axis, parallel to the diagonal line $y = x$. If $S < 0$, maximum growth requires $\alpha = -\beta$, and so the lines of constant phase are parallel to $y = -x$. Accordingly, the general condition of instability is

$$2\mu|S|\, h > T, \tag{6}$$

which means $|N_{xy}| > T$; and when (6) is satisfied, the waveform with maximum growth is shown by (5) to have wavelength $\lambda_m = 2\pi/k_m$ given by

$$\lambda_m = \pi\left\{\frac{2(2\mu|S|\,h-T)}{g\rho_2}\right\}^{\frac{1}{2}}. \tag{7}$$

Note that λ_m is indefinitely small when the instability condition (6) is just satisfied.

The simple theory thus predicts that incipient buckling in a thin viscous layer undergoing shear should appear as ripples with extremely small wavelengths and crests inclined at 45° to the direction of the primary motion. The small-λ_m result supports the contention that a local criterion suffices without regard to boundary conditions. On the other hand, this result grossly violates the condition $k_m h \ll 1$ which would justify the membrane approximations underlying (3). The theoretical predictions are not self-consistent, therefore, and it can be expected that the result (6) generally *underestimates* the value of $|S|$ needed for buckling. This deficiency was noted by Suleiman & Munson (1981, p. 5) in comparing their experimental results with the (implicit) suggestion by Taylor (1969) that (6) might be the criterion of buckling instability. Although they did not propose a rational improvement upon (6), they found that the empirical criterion mentioned in §1 gave a much better correlation of their results. The theory in §3 is freed from membrane approximations, so avoiding the inconsistent estimate (7) for λ_m and providing a more reliable estimate of the buckling condition.

It is noteworthy, however, that Taylor (1969, p. 388) recorded experimental observations in apparent agreement with the simple theory. A horizontal disk of 55 mm diameter was partly immersed in a layer of golden syrup, 10 mm deep, floating on carbon tetrachloride contained in a vessel of 150 mm diameter. As the disk was rotated the surface of the syrup was observed to remain flat until the angular speed was raised to 0.37 r.p.s. At this speed, ripples appeared in the surface close to the rim of the disk, where the shearing rate imposed on the syrup was largest; their crests were inclined at 45° to the rim and their wavelength was extremely small. The possibility of a skin with some rigidity having formed was mentioned by Taylor; but he noted as counter-evidence that the surface flattened leaving no sign of the wave pattern in a few seconds after the rotation had been stopped. He wisely added, 'It may well be that some surface viscosity is present.'

This suggestion was convincingly confirmed by some simple tests made by one of us many years ago. Annular layers of golden syrup were observed under shearing in an apparatus much the same as Taylor's (1969, figures 15–17). When the apparatus had been left closed over the top for a day or more, no buckling could be induced in the form reported by Taylor. On the other hand, when the apparatus had been left open for a comparable time, the surface could be crinkled into tiny ripples by moderate rates of shearing, however deep the layer of syrup. Presumably the exposure to dry air in the second case had allowed water to evaporate from the surface of the syrup, leaving a skin of more concentrated, nearly crystalline sugar which buckled more or less independently of the less viscous liquid below. In prolonged contact with saturated air in the closed apparatus, the surface evidently lost any such skin.

3. Improved theory

The aim is to estimate the condition for the onset of buckling more reliably than by the simple theory, for comparison with the experimental results presented later. As before, we consider a layer of thickness $2h$ composed of liquid with density ρ_1 and large viscosity μ, which floats on a liquid with density $\rho_2 > \rho_1$. The second liquid is taken to be immiscible with the first, so that the interface has a positive surface tension T_2, and the upper surface of the viscous liquid is taken to be free with surface tension T_1. The motion is assumed to be slow enough and the viscosity of the second liquid small enough for hydrodynamic effects in it to be negligible.

Take axes (x, y, z) with origin at the centre of the layer and z vertical upwards, so that the upper horizontal surface of the undisturbed layer is described by $z = h$ and the lower by $z = -h$. The layer is taken to be sheared at a rate $S > 0$, which will be treated as a constant, and so the primary motion can be represented by

$$(u, v, w) = (Sy, 0, 0). \tag{8}$$

The stability of this motion is to be examined on the assumption that μ is large enough for inertial effects to be negligible; specifically, $\rho_2 Sh^2/\mu \ll 1$.

In the perturbed motion the upper and lower surfaces of the viscous layer are described respectively by

$$\left.\begin{aligned} z &= h + \zeta_1(x, y, t), \\ z &= -h + \zeta_2(x, y, t), \end{aligned}\right\} \tag{9}$$

where ζ_1 and ζ_2 are infinitesimal. Focusing on a generic Fourier component of the perturbation, we consider

$$\begin{aligned} \zeta_i &= \epsilon_i(t) \cos\{\alpha(x - Syt) - \beta_0 y\} \\ &= \epsilon_i(t) \cos(\alpha x - \beta y) \quad (i = 1, 2), \end{aligned} \tag{10}$$

with
$$\beta = \beta_0 + \alpha St. \tag{11}$$

Here α is a real constant, but β is a real function of time t, likewise $k = (\alpha^2 + \beta^2)^{\frac{1}{2}} > 0$ and $\theta = \arctan(\beta/\alpha)$. As illustrated in figure 1, lines of constant phase in the waves described by (10) and (11) are rotated by the primary motion, remaining coincident with the same liquid particles. The advantage of this representation is that the linearized kinematic conditions at the two surfaces, namely

$$\frac{\partial \zeta_i}{\partial t} + Sy\frac{\partial \zeta_i}{\partial x} = w(x, y, \pm h, t),$$

reduce to
$$\dot{\epsilon}_i = \hat{w}(\pm\gamma) \quad (i = 1, 2), \tag{12}$$

with $\gamma = kh$, when the vertical velocity w is written

$$w = \hat{w}(kz) \cos(\alpha x - \beta y). \tag{13}$$

In (12) $\dot{\epsilon}_i$ denotes $\mathrm{d}\epsilon_i/\mathrm{d}t$, and this pair of equations will be the only place in the formulation where time-derivatives occur. Thus, in the solution of the hydrodynamic equations that follows, the time-dependent quantities β, k and θ can be treated as if they were constant parameters.

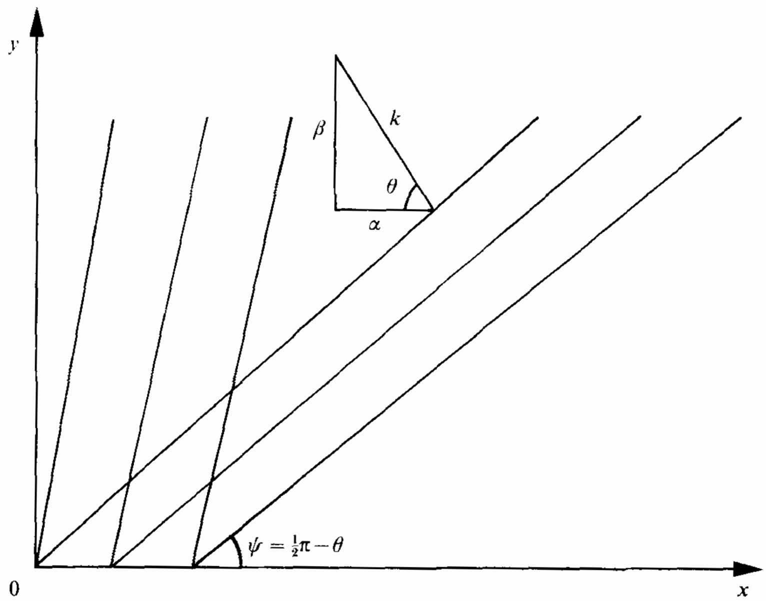

FIGURE 1. Definition sketch illustrating evolution of lines of constant phase in the horizontal (x, y)-plane.

3.1. *Dynamical equations*

In terms of the velocity vector $\boldsymbol{u} = (u, v, w)$ and $p^* = p + g\rho_1 z$, where p is pressure, the equations of motion for an incompressible Newtonian liquid without inertia are

$$\mu\Delta\boldsymbol{u} = \nabla p^*, \tag{14}$$

$$\nabla\cdot\boldsymbol{u} = 0, \tag{15}$$

where $\Delta \equiv \partial_x^2 + \partial_y^2 + \partial_z^2$. Because of (15), taking the divergence of (14) shows that

$$\Delta p^* = 0, \tag{16}$$

whence (14) also implies that $\Delta^2\boldsymbol{u} = 0$, in particular

$$\Delta^2 w = 0. \tag{17}$$

It will be convenient to formulate the boundary-value problem in terms of w as expressed by (13). The horizontal velocity components u and v, which too are biharmonic functions of (x, y, z), are not needed explicitly. Corresponding to the expression (13) for w, they can be seen from (15) to be both proportional to $\hat{w}'(kz)$ $\sin(\alpha x - \beta y)$; but their respective amplitudes depend on the tangential-stress conditions at the upper and lower boundaries (cf. (20) below) as well as on (15).

The general solution of (17) in the form (13) has

$$\hat{w} = A\cos Z + BZ\sinh Z + C\cosh Z + DZ\sinh Z, \tag{18}$$

where $Z = kz$ and A, B, C, D are constants or functions of time alone. Note that the terms with coefficients A and B are even in z, so representing a vertical displacement of the layer as a whole, whereas the terms with coefficients C and D are odd in z and so represent a thickening or contraction of the layer. Writing $p^* = \hat{p}^*(Z) \cos(\alpha x - \beta y)$, we find at once from (18) and the z-component of (14) that

$$\hat{p}^* = 2\mu k(B \sinh Z + D \cosh Z), \tag{19}$$

and thus p^* is confirmed to satisfy (16).

3.2. *Boundary conditions*

In addition to the kinematic conditions (12), linearized boundary conditions referring to tangential and normal stress will complete the determination of the solution in the form (10). Write τ_{ij} for the stress tensor, noting that in the primary state its only non-zero components are $\tau_{12} = \tau_{21} = \mu S$ and $\tau_{33} = g\rho_2(z-h)$. For the perturbed motion, the components include $\tau_{13} = \mu(u_z + w_x)$ and $\tau_{23} = \mu(v_z + w_y)$. To first order in infinitesimals, the upwardly directed unit normal to either of the surfaces (9) is given by $\boldsymbol{n} = (-\zeta_x, -\zeta_y, 1)$, where ζ denotes ζ_1 or ζ_2 respectively. These surfaces are assumed to be free, supporting no tangential component of stress; thus $\tau_{ij} n_j$ evaluated at either surface is required to have no tangential component, or equivalently

$$\tau_{ij} n_j - \tau_{jk} n_j n_k n_i = 0$$

for all $i = 1, 2, 3$. Using the facts just noted, we find that to first order this condition reduces to

$$u_z + w_x = S\zeta_y, \quad v_z + w_y = S\zeta_x, \tag{20}$$

where the partial derivatives of the velocities are evaluated at $z = \pm h$ and ζ denotes ζ_1 or ζ_2 respectively.

The elimination of u and v by cross-differentiation of (20) and use of (15) gives

$$w_{xx} + w_{yy} - w_{zz} = 2S\zeta_{xy},$$

whence substitution of (13) for w and (10) for ζ leads to the pair of boundary conditions for $\hat{w}(Z)$

$$\begin{aligned} \hat{w}''(\pm\gamma) + \hat{w}(\pm\gamma) &= (2S\alpha\beta/k^2)\,\epsilon_i \\ &= (S \sin 2\theta)\,\epsilon_i \quad (i = 1, 2). \end{aligned} \tag{21}$$

(Recall that $\gamma = kh$.) Putting the general solution (18) for $\hat{w}$ into (21) and writing for short $\mathrm{c} = \cosh\gamma$, $\mathrm{s} = \sinh\gamma$, we obtain

$$A\mathrm{c} + B(\mathrm{c} + \gamma\mathrm{s}) \pm [C\mathrm{s} + D(\mathrm{s} + \gamma\mathrm{c})] = \tfrac{1}{2}(S \sin 2\theta)\,\epsilon_i,$$

the addition and subtraction of which gives

$$\left.\begin{aligned} A\mathrm{c} + B(\mathrm{c} + \gamma\mathrm{s}) &= \tfrac{1}{2}(S \sin 2\theta)\,\xi, \\ C\mathrm{s} + D(\mathrm{s} + \gamma\mathrm{c}) &= \tfrac{1}{2}(S \sin 2\theta)\,\eta, \end{aligned}\right\} \tag{22}$$

with

$$\xi = \tfrac{1}{2}(\epsilon_1 + \epsilon_2), \qquad \eta = \tfrac{1}{2}(\epsilon_1 - \epsilon_2).$$

To express normal-stress conditions, linearized approximations to the curvatures of the surfaces (9) are used. Thus, allowing for the normal-stress discontinuity due to surface tension, we have to first order

$$p - 2\mu w_z = -T_1(\partial_x^2 + \partial_y^2)\,\zeta_1 = k^2 T_1\,\zeta_1$$

at $z = h + \zeta_1$, and accordingly

$$p^* - 2\mu w_z = (g\rho_1 + k^2 T_1)\,\zeta_1$$

at $z = h$. Hence the substitution of (13) for w, (18) for $\hat{w}$ and (19) for $\hat{p}^*$ leads to

$$A\mathrm{s}+B\gamma\mathrm{c}+C\mathrm{c}+D\gamma\mathrm{s} = -\frac{(g\rho_1+k^2T_1)}{2\mu k}\epsilon_1. \tag{23}$$

The pressure on the *lower* side of the interface $z = -h+\zeta_2$ is accountable as hydrostatic pressure in the heavier liquid beneath, so being given by $2gh\rho_1 - g\rho_2\zeta_2$. We therefore have

$$p^* - 2\mu w_z = -\{g(\rho_2-\rho_1)+k^2T_2\}\zeta_2,$$

and substitution for w and p^* as before leads to

$$A\mathrm{s}+B\gamma\mathrm{c}-C\mathrm{c}-D\gamma\mathrm{s} = -\frac{\{g(\rho_2-\rho_1)+k^2T_2\}}{2\mu k}\epsilon_2. \tag{24}$$

Addition and subtraction of (23) and (24) give

$$\left.\begin{aligned} A\mathrm{s}+B\gamma\mathrm{c} &= -Q\xi-R\eta, \\ C\mathrm{c}+D\gamma\mathrm{s} &= -R\xi-Q\eta, \end{aligned}\right\} \tag{25}$$

in which
$$Q = \frac{g\rho_2+k^2(T_1+T_2)}{4\mu k}$$

and
$$R = \frac{g(2\rho_1-\rho_2)+k^2(T_1-T_2)}{4\mu k}.$$

Finally, let us substitute (18) for $\hat{w}$ into the kinematic conditions (12), which thus provide

$$\left.\begin{aligned} \dot{\xi} &= A\mathrm{c}+B\gamma\mathrm{s}, \\ \dot{\eta} &= C\mathrm{s}+D\gamma\mathrm{c}. \end{aligned}\right\} \tag{26}$$

3.3. *Equations for ξ and η*

The coefficients A, B, C, D can be found in terms of ξ and η by solution of the four equations (22) and (25). Thus (26) is reducible to a linear system of ordinary differential equations for $\xi(t)$ and $\eta(t)$. The result is

$$\left.\begin{aligned} \dot{\xi} &= a_{11}\xi+a_{12}\eta, \\ \dot{\eta} &= a_{21}\xi+a_{22}\eta, \end{aligned}\right\} \tag{27}$$

with
$$\left.\begin{aligned} a_{11} &= \frac{\frac{1}{2}\gamma S\sin 2\theta - \mathrm{c}^2Q}{\mathrm{sc}-\gamma}, \quad a_{12} = -\frac{\mathrm{c}^2R}{\mathrm{sc}-\gamma}, \\ a_{21} &= -\frac{\mathrm{s}^2R}{\mathrm{sc}+\gamma}, \quad a_{22} = -\frac{\frac{1}{2}\gamma S\sin 2\theta+\mathrm{s}^2Q}{\mathrm{sc}+\gamma}. \end{aligned}\right\} \tag{28}$$

These four coefficients are all complicated functions of t. But, as will be discussed below, plausible conclusions about the stability of the sheared layer can be based on a study of instantaneous values of the coefficients for given k and θ. First, however, the following simple checks on (27) and (28) deserve to be noted.

(i) To cover the case of a very deep layer, take the limit $\gamma \to \infty$. The direct effect of S on (27) disappears in the limit, which reduces the system to

$$\dot{\xi} = -Q\xi-R\eta, \quad \dot{\eta} = -R\xi-Q\eta.$$

Because $\xi+\eta=\epsilon_1$ and $\xi-\eta=\epsilon_2$, the reduced system is equivalent to the uncoupled equations

$$\left.\begin{aligned}\dot{\epsilon}_1 &= -(Q+R)\,\epsilon_1 = -\left\{\frac{g\rho_1+k^2T_1}{2\mu k}\right\}\epsilon_1,\\ \dot{\epsilon}_2 &= -(Q-R)\,\epsilon_2 = -\left\{\frac{g(\rho_2-\rho_1)+k^2T_2}{2\mu k}\right\}\epsilon_2.\end{aligned}\right\}$$

These results correctly demonstrate the damping rates for waves on the upper free surface and for waves on the lower interface (cf. Lamb 1932, p. 628). As obviously to be expected, it is confirmed that in the limit the two classes of waves are independent and the respective damping rates depend on k but not on θ. Note, however, that a purely kinematic effect of shearing is still demonstrated because the preceding results are valid with $k=\{\alpha^2+(\beta_0+\alpha St)^2\}^{\frac{1}{2}}$.

(ii) Take the case $\gamma \ll 1$, for which $\mathrm{sc}-\gamma \doteqdot \frac{2}{3}\gamma^3$ and $\mathrm{sc}+\gamma \doteqdot 2\gamma$. As first approximations for small γ, we have

$$\left.\begin{aligned}a_{11} &= \frac{3}{2\gamma^3}(\tfrac{1}{2}\gamma S\sin 2\theta - Q)\\ &= \frac{3}{8\mu h^3k^2}\left\{2\mu hS\sin\theta - \frac{g\rho_2}{k^2}-(T_1+T_2)\right\},\\ a_{22} &= -\tfrac{1}{4}(S\sin 2\theta + 2\gamma Q)\end{aligned}\right\} \tag{29}$$

and $$a_{12}a_{21} = 3R^2/4\gamma^2 \ll a_{11}^2.$$

In view of the last inequality and because $|a_{22}| \ll |a_{11}|$ outside a narrow range of k and θ where a_{11} is exceptionally small, a good general estimate of the highest eigenvalue of a_{ij} is just a_{11} in the present case. Thus (29) recovers the result (5) for growth rate according to the simple theory, which we have shown in §2 to be suspect because the supposition $\gamma \ll 1$ is inconsistent with the choice of k maximizing the expression (29).

(iii) Take $Q=R=0$, in which case the perturbed layer suffers no restoring force. According to (27) and (28), the modes ξ and η are then uncoupled, as can be expected from considerations of symmetry. Assuming $S>0$, we have that $\dot{\xi}/\xi>0$ but $\dot{\eta}/\eta<0$ when $0<\theta<\frac{1}{2}\pi$. That is, when $0<\psi<\frac{1}{2}\pi$, where $\psi=\frac{1}{2}\pi-\theta$ is the angle between the x-axis and constant-phase lines (see figure 1), waves of bending are amplified (i.e. the layer buckles) but waves of successive thickening and thinning are damped. Conversely, when $\frac{1}{2}\pi<\psi<\pi$, we have $\dot{\xi}/\xi<0$ but $\dot{\eta}/\eta>0$. Thus waves of thickening and thinning are amplified in this case, although their rate of growth $-\frac{1}{2}(\gamma S\sin 2\psi)/(\mathrm{sc}+\gamma)>0$ is comparatively small if γ is small. All these conclusions accord with intuition.

If $\gamma \ll 1$, first approximations to the differential equations for ξ and η with $Q=R=0$ are

$$\frac{\dot{\xi}}{\xi}=\frac{3S\sin 2\theta}{4\gamma^2},\quad \frac{\dot{\eta}}{\eta}=-\tfrac{1}{4}S\sin 2\theta, \tag{30}$$

which can easily be solved. Recalling (11), consider

$$\tau=\tan\theta=\cot\psi=\beta/\alpha=\tau_0+St,$$

whence $$\gamma=kh=\alpha h(1+\tau^2)^{\frac{1}{2}}=\alpha h\{1+(\tau_0+St)^2\}^{\frac{1}{2}},$$

$$\sin 2\theta=\frac{2\tau}{1+\tau^2}=\frac{2(\tau_0+St)}{1+(\tau_0+St)^2}.$$

Here τ_0 is short for $\tau(0)$, which may take any real value. After substitution of these expressions into the right sides of (30), the solutions are found to be respectively

$$\frac{\xi(t)}{\xi(0)} = \exp\left[\frac{3}{4\alpha^2h^2}\left(\frac{1}{1+\tau_0^2} - \frac{1}{1+(\tau_0+St)^2}\right)\right], \tag{31}$$

$$\frac{\eta(t)}{\eta(0)} = \left[\frac{1+\tau_0^2}{1+(\tau_0+St)^2}\right]^{\frac{1}{4}}. \tag{32}$$

These solutions remain good approximations to the solutions of the exact linear problems only while γ remains small. Eventually, when the phase-lines are rotated to become nearly enough parallel with the x-axis, the underlying assumption $\gamma \ll 1$ is violated.

Our general conclusions are borne out conspicuously by (31) and (32). If $\tau_0 < 0$ (i.e. the phase-lines initially point in a direction between north and west in figure 1), ξ is shown to decrease rapidly and η to increase much more slowly during the interval $[0, -\tau_0/S)$. At $t = -\tau_0/S$, when the phase-lines point northward, ξ is a minimum and η a maximum. Thereafter ξ rapidly increases and η slowly decreases.

(It should be acknowledged that, as a putative approximation for $\gamma \ll 1$, the differential equation $\dot{\xi} = a_{11}\xi$ with a_{11} expressed by (29) can be solved explicitly without difficulty. For the reasons explained in §2, however, such an approximation is misleading as regards the stability problem, and therefore we pass over the solution.)

3.4. *Conditions for instability*

Typically γ is fairly small, so that $|a_{11}| \gg |a_{22}|$ and $|a_{12}| \gg |a_{21}|$ in (27). Therefore a simple estimate of the buckling condition is that $a_{11} > 0$ for some γ and θ. Because a_{11} is largest for $\theta = \frac{1}{4}\pi$, the estimated condition amounts to $S > S_c$, where according to the first of (28)

$$S_c = 2 \min_{\gamma} (c^2Q/\gamma),$$

that is,

$$S_c = \frac{1}{2\mu} \min_{\gamma}\left(\frac{g\rho_2 h}{\gamma^2} + \frac{T}{h}\right)\cosh^2\gamma. \tag{33}$$

(Here T is written for T_1+T_2.) In terms of the dimensionless measures of shear stress and layer thickness

$$f = \mu S/(g\rho_2 T)^{\frac{1}{2}}, \quad H = 2h(g\rho_2/T)^{\frac{1}{2}}, \tag{34}$$

the buckling condition becomes $f > f_c$ with

$$f_c = \min_{\gamma}\left(\frac{H}{4\gamma^2} + \frac{1}{H}\right)\cosh^2\gamma. \tag{35}$$

Although plainly a great improvement on the primitive result $f_c = 1/H$ represented in (6), the expression (35) is a slight overestimate of f_c, to be corrected below. Note the tentative but plausible basis of the estimate (35). We reason that when in practice $f > f_c$ and (27) has a solution ξ growing comparatively rapidly for θ near $\frac{1}{4}\pi$ and γ near the minimizer of the expression (35), then buckling should appear locally provided the lateral (horizontal) extent of the layer is great enough for boundary conditions at its edges to be unimportant.

Treating the matrix on the right side of (27) as constant, we note that the system then has two solutions in the form

$$(\xi, \eta) = (\xi(0), \eta(0)) \exp \lambda_i t,$$

where the λ_i ($i = 1, 2$), the eigenvalues of the matrix, are given by

$$\lambda_i = \tfrac{1}{2}\{a_{11} + a_{22} \pm [(a_{11} - a_{22})^2 + 4a_{12}a_{21}]^{\frac{1}{2}}\}.$$

A condition of marginal stability is indicated by one of the λ_i vanishing, that is, by

$$M = a_{11}a_{22} - a_{12}a_{21} = 0,$$

which on substitution from (28) and cancellation of a factor $(\mathrm{s}^2\mathrm{c}^2 - \gamma^2)^{-1} > 0$ gives

$$-\tfrac{1}{4}(\gamma S \sin 2\theta)^2 + \tfrac{1}{2}Q(\gamma S \sin 2\theta) - \mathrm{s}^2\mathrm{c}^2(Q^2 - R^2) = 0. \tag{36}$$

The positive root of (36) is

$$\begin{aligned}\gamma S \sin 2\theta &= [Q^2 + 4\mathrm{s}^2\mathrm{c}^2(Q^2 - R^2)]^{\frac{1}{2}} + Q \\ &= Q\{(\cosh^2 2\gamma - r^2 \sinh^2 2\gamma)^{\frac{1}{2}} + 1\},\end{aligned}$$

where $r = R/Q < 1$. Hence the critical value of f, above which (27) has a rapidly growing solution for θ near $\frac{1}{4}\pi$, is found to be given by

$$f_\mathrm{c} = \tfrac{1}{2} \min_{\gamma} \left(\frac{H}{4\gamma^2} + \frac{1}{H}\right)\{(\cosh^2 2\gamma - r^2 \sinh^2 2\gamma)^{\frac{1}{2}} + 1\}. \tag{37}$$

Note that (37) reduces to (35) in the case $r = 0$, but for $0 < r < 1$ the value of f_c given by (37) is the smaller. As will be shown in §5, however, estimates of f_c based on (37) with experimental parameter values are little different from estimates based on (35).

It remains to confirm that (27) has a rapidly growing solution when $f > f_\mathrm{c}$, with f_c given by (37). First, however, we should note that the negative root of (36) is

$$\begin{aligned}\gamma S \sin 2\theta &= -[Q^2 + 4\mathrm{s}^2\mathrm{c}^2(Q^2 - R^2)]^{\frac{1}{2}} + Q \\ &= -Q\{(\cosh^2 2\gamma - r^2 \sinh^2 2\gamma)^{\frac{1}{2}} - 1\},\end{aligned}$$

whence it appears that (27) has a growing solution for θ near $-\frac{1}{4}\pi$ when $f > f_\mathrm{c}^-$, where

$$f_\mathrm{c}^- = \tfrac{1}{2} \inf_{\gamma} \left(\frac{H}{4\gamma^2} + \frac{1}{H}\right)\{(\cosh^2 2\gamma - r^2 \sinh^2 2\gamma)^{\frac{1}{2}} - 1\}. \tag{38}$$

The infimum specified here is approached in the limit $\gamma \to 0$. In keeping with the discussion in §3.3(iii), the disturbances thus indicated to grow when $f > f_\mathrm{c}^-$ are long waves of thickening and thinning, whose growth rates are presumably small compared with the buckling mode that grows when $f > f_\mathrm{c}$.

To exhibit this essential difference, let us consider the exponent λ_1 that becomes positive when $M < 0$ and work out its rate of increase with f above f_c and f_c^- respectively. Because each exponent λ_i satisfies $\lambda^2 - (a_{11} + a_{22})\lambda + M = 0$, we have

$$\left(\frac{\mathrm{d}\lambda_1}{\mathrm{d}f}\right)_\mathrm{c} = \left(\frac{1}{a_{11} + a_{22}} \frac{\mathrm{d}M}{\mathrm{d}f}\right)_\mathrm{c}.$$

Also, by differentiation of (36), we have

$$\left(\frac{\mu^2}{g\rho_2 T}\right)\left(\frac{\mathrm{d}M}{\mathrm{d}f}\right)_\mathrm{c} = -\frac{\frac{1}{2}\gamma(\gamma f_\mathrm{c} - \bar{Q}_\mathrm{c})}{\mathrm{s}^2\mathrm{c}^2 - \gamma^2},$$

where $\bar{Q} = \mu Q/(g\rho_2 T)^{\frac{1}{2}}$, and from (28)

$$[\mu/(g\rho_2 T)^{\frac{1}{2}}](a_{11}+a_{22})_c = -\{\bar{Q}_c(\gamma+s^3c+sc^3)-\gamma^2 f_c\}/(s^2c^2-\gamma^2).$$

Hence, respective to the buckling value f_c given by (37), the result is

$$\frac{(g\rho_2 T)^{\frac{1}{2}}}{\mu}\left(\frac{d\lambda_1}{df}\right)_c \equiv \left(\frac{d\lambda_1}{dS}\right)_c = \frac{\frac{1}{2}(\cosh^2 2\gamma - r^2\sinh^2 2\gamma)^{\frac{1}{2}}}{(4\gamma)^{-1}\sinh 4\gamma - (\cosh^2 2\gamma - r^2\sinh^2 2\gamma)^{\frac{1}{2}}}, \tag{39}$$

in which γ should be given its value minimizing the right-hand side of (37). Because the denominator of (39) is $O(\gamma^2)$ as $\gamma \to 0$, the quotient takes large values when γ is fairly small.

In contrast, the corresponding result respective to the critical condition given by (38) is

$$\left(\frac{d\lambda_1}{dS}\right)_c = \frac{\frac{1}{2}(\cosh^2 2\gamma - r^2\sinh^2 2\gamma)^{\frac{1}{2}}}{(4\gamma)^{-1}\sinh 4\gamma + (\cosh^2 2\gamma - r^2\sinh^2 2\gamma)^{\frac{1}{2}}}, \tag{40}$$

which takes its largest value $\frac{1}{4}$ in the limit $\gamma \to 0$ relevant to (38). For any γ, the right side of (39) is larger than the right side of (40), greatly so when γ is small. Although a secondary, non-buckling instability is indicated when $f > f_c^-$, which condition is generally satisfied well below the buckling condition (37), growth rates for the amplified waves of thickening and thinning seem to be too small for the waves to be discernible in practice. Such waves were not noticed in the experiments.

4. Experimental apparatus

The apparatus is illustrated in figure 2. In it layers of highly viscous liquid were observed in shearing motion between the rim of a rotating circular disk made of aluminium, 20 mm thick, and the concentric inner wall of a circular cylindrical container made of Perspex. A steel shaft passing centrally through the disk and fixed to it was supported by two bearings, one in the base of the container and the other in the lid, which was removable but tightly fitting. The disk was rotated at constant angular speed Ω by a d.c. motor coupled to the shaft through a 50:1 reduction gear. Stabilized by feedback control of the motor, the speed was continuously adjustable over a wide range.

The rim of the rotating disk had radius $R_1 = 140 \pm 0.1$ mm, and the inner wall of the container had radius $R_2 = 185 \pm 0.1$ mm. Thus the width of the annular gap between the moving rim and the stationary wall was 45 mm, which we judged large enough for menisci to have insignificant effects on the liquid surfaces spanning the annulus.

With the axis of symmetry carefully adjusted to be vertical, the container was filled with distilled water to a level just above the lower edge of the aluminium disk. Silicone oil, having specific gravity 0.978, was then gently poured onto the water surface to float as an annular layer with its inner edge on the rim of the disk and its outer edge on the wall of the container. Each experimental run taking several days was begun with the layer of silicone oil at its thickest. After the critical speed for buckling at this thickness had been measured, a small quantity of the oil was removed and eventually, when the thinner layer had fully settled into a uniform state, the second measurement of critical speed was made. This procedure was repeated many times until the layer became so thin that it was ruptured in the attempt to remove more of the oil. Settling times typically as long as 24 hrs were allowed after each reduction of the oil layer, and they were found sufficient for the

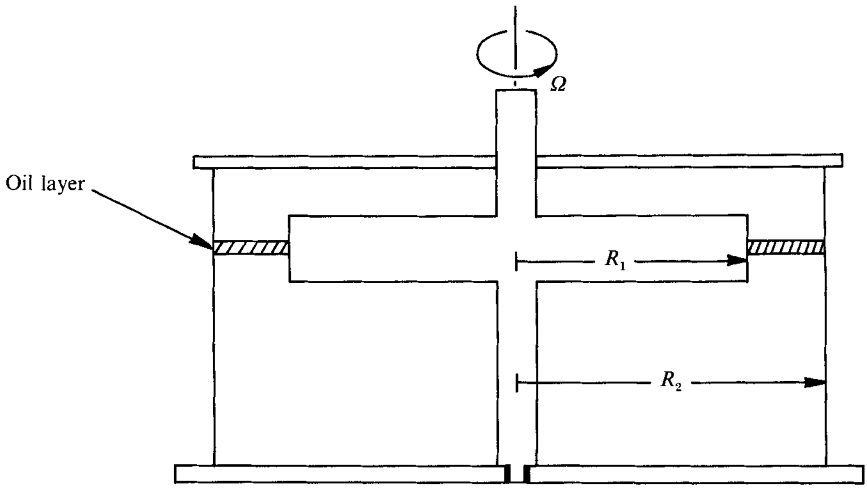

FIGURE 2. Schematic cross-section of apparatus.

disappearance of any air or water bubbles that happened to be entrained in the layer.

The thickness $2h$ of the layer was measured by means of a depth gauge controlled by a micrometer, which moved a fine needle vertically through the layer. Observed through a microscope, contact between the point of the needle and either the upper surface or the interface with the water below could be discerned confidently. The measurements of $2h$ in this way were estimated to be accurate within ± 0.04 mm.

In dealing with capillary effects on the stability of a sheared layer of viscous liquid, our theory has revealed the primary importance of the sum $T = T_1 + T_2$, where T_1 is the surface-tension coefficient for the upper interface between the oil and air and T_2 that for the lower interface between the oil and water. Adopting a good approximation explained by Davies & Rideal (1961, p. 31) to apply generally to immiscible liquids, which was also adopted by Suleiman & Munson (1981, p. 2), we assume $T_2 = T_2' - T_1$ and hence $T = T_2'$, where T_2' is the surface tension of water exposed to air. Thus we take $T = 72.8$ dyn/cm ($\equiv 72.8$ mN/m), the value of surface tension for water at 20 °C.

On the assumptions that the annular layer of highly viscous liquid is uniform and that hydrodynamic effects in the water below it are negligible, its circumferential velocity V varies with radius r according to

$$V = \frac{\Omega R_1^2}{R_2^2 - R_1^2}\left(\frac{R_2^2}{r} - r\right).$$

The shear stress in the layer is therefore $-\mu S$ with

$$S = -\frac{\mathrm{d}V}{\mathrm{d}r} + \frac{V}{r} = \frac{2\Omega R_1^2 R_2^2}{(R_2^2 - R_1^2)\, r^2}.$$

The largest value of S, at $r = R_1$, is given by

$$S_{\mathrm{m}} = \frac{2\Omega R_2^2}{R_2^2 - R_1^2}, \tag{41}$$

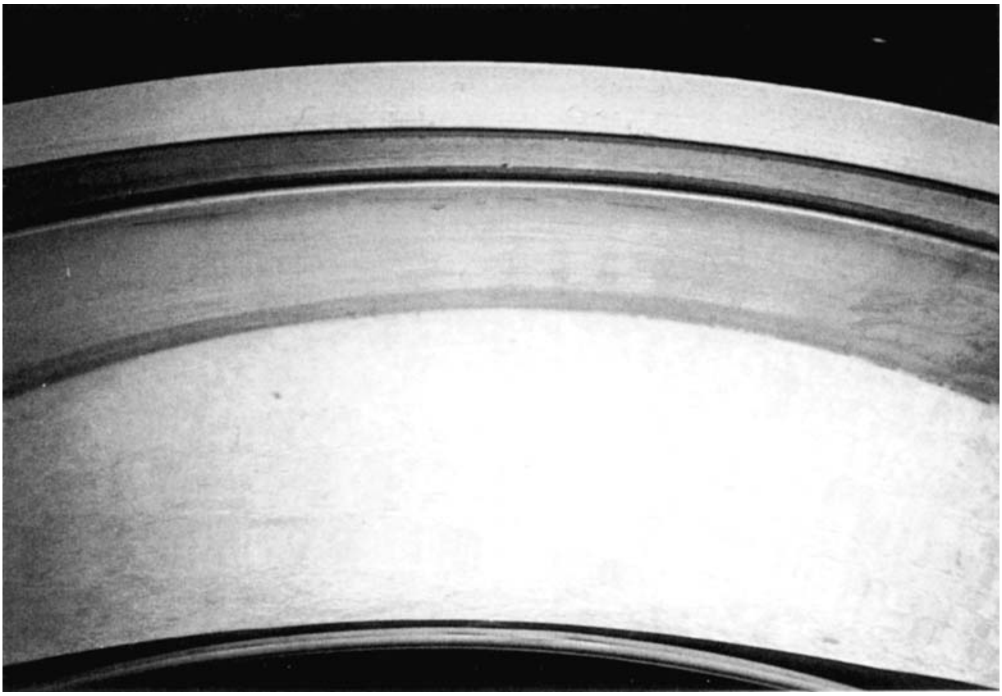

(a)

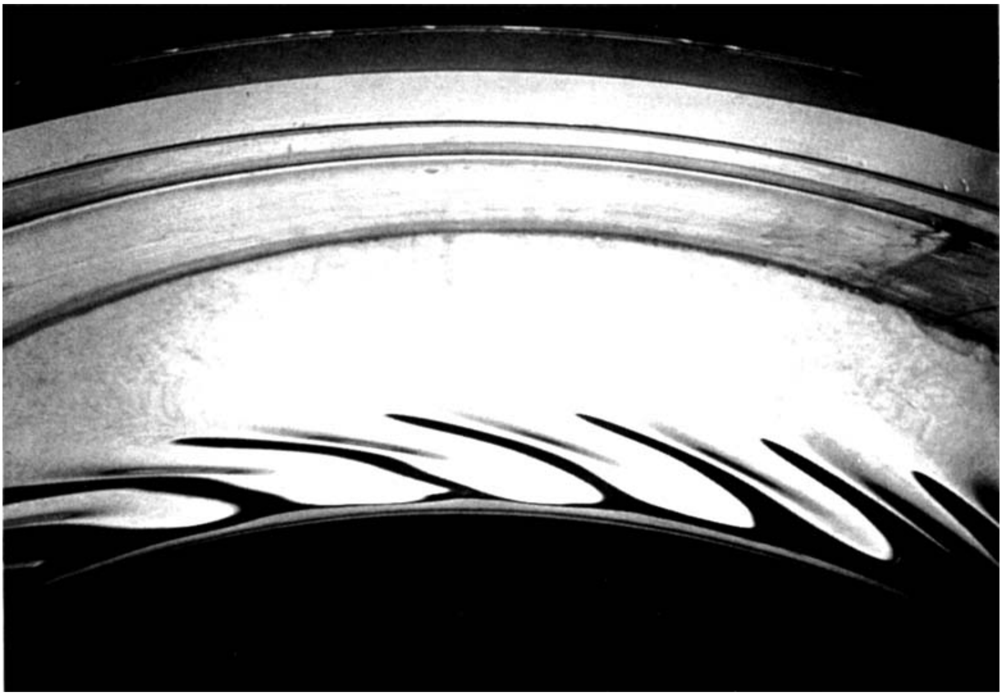

(b)

FIGURE 3. Photographs of sheared layer from above: (a) at critical angular velocity; (b) at angular velocity 10% greater than critical.

which formula will be used to reduce the observed critical values of Ω; and the least value of S, taken at the outer edge $r = R_2$, is $(R_1/R_2)^2 = 0.573$ times S_m. The change in S across the gap is thus large enough for the first signs of buckling to be expected distinctly near to the inner edge of the layer.

Three silicone oils were used in the experiments, having viscosities $\mu = 10000$, 30770 and 64000 cP measured by a Sangymo Weston rheogoniometer. This instrument was also used to estimate non-Newtonian effects in the liquids, specifically to measure normal-stress differences caused by simple shearing. At shearing rates typical of our experiments, such effects were checked to be insignificant in the first two, less viscous oils. They were significant in the oil with viscosity 64000 cP, however, being directly observable in our apparatus as a thickening of the sheared layer at its inner edge: that is, Weissenberg effects were noticeable.

5. Experimental results

Having been left long enough to settle into its uniform horizontal configuration, a layer of silicone oil was observed to remain featureless until the speed Ω of the rotating disk was raised to a critical value Ω_c, which depended on the layer's thickness $2h$ and viscosity μ. At the critical speed ripples appeared close to the rim of the disk, with crests inclined at approximately 45° to the circular paths of the liquid particles. When Ω was raised to 5% or more above Ω_c, the ripples became much more prominent; both their amplitude and their radial extent increased steadily with $\Omega - \Omega_c > 0$, and the angle between their crests and the particle paths fell progressively further below 45°. Photographs showing a layer just at and well above the critical condition are presented in figure 3.

The onset of buckling was difficult to detect by direct observation, and to refine the estimates of Ω_c the following method was adopted. The layer of silicone oil was illuminated from below by diffused light, and an image of its upper surface was projected onto the ceiling. In a darkened room, the first appearance of a regular pattern of shadows in the image was found to be a sensitive indicator of incipient buckling.

For each layer with a particular thickness $2h$ and viscosity μ, the speed Ω was increased in small steps until ripples were detected. We then repeated the procedure taking finer steps to approach the critical value Ω_c. The estimate was checked several times, both by gradual increase in Ω from below and by gradual decreases from above. No hysteresis was discovered, and the measurements of Ω_c were found to be repeatable within about 1% in successive experiments from day to day.

Results for the silicone oils with viscosities 10100 and 30770 cP are presented in figures 4 and 5. Estimated critical values of the dimensionless shear stress $f = \mu S/(g\rho_2 T)^{\frac{1}{2}}$ (cf. (34) in §3.4), with S evaluated by substituting measurements of Ω_c in (41), are plotted against dimensionless thickness $H = 2h(g\rho_2/T)^{\frac{1}{2}}$. Theoretical curves of f_c versus H according to (35) and (37) are also shown. The curve according to (37), drawn dashed in figure 4, was found by use of the value 23.8 dyn/cm given by the manufacturer for the surface tension of the silicone oil (T_1 is needed to evaluate the coefficient r in (37)); and except at the highest values of H this curve can be seen to be practically the same as that according to (35). As demonstrated by figures 4 and 5, the agreement between theory and experiment is satisfactory. In particular, the prediction that the critical shear stress has a minimum as a function of H is borne out plainly by these experimental results.

Corresponding results for the silicone oil with viscosity 64000 cP are presented in

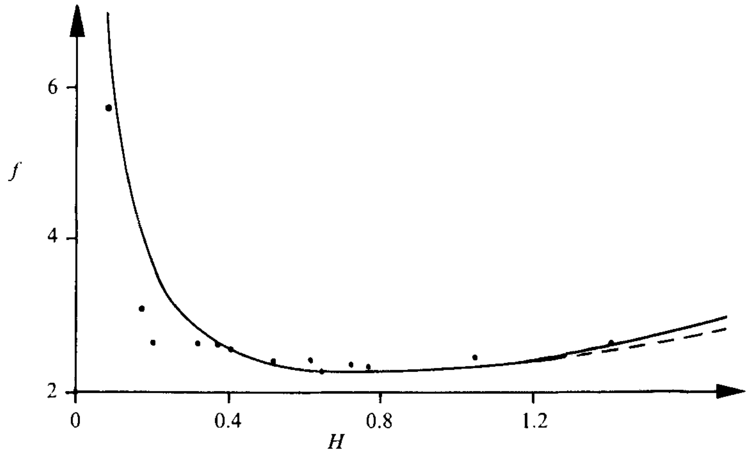

FIGURE 4. Measured critical values of $f = \mu S/(g\rho_2 T)^{\frac{1}{2}}$ plotted against $H = 2h(g\rho_2/T)^{\frac{1}{2}}$, for silicone oil with viscosity 10000 cP. Theoretical prediction is continuous curve according to (35), dashed curve according to (37).

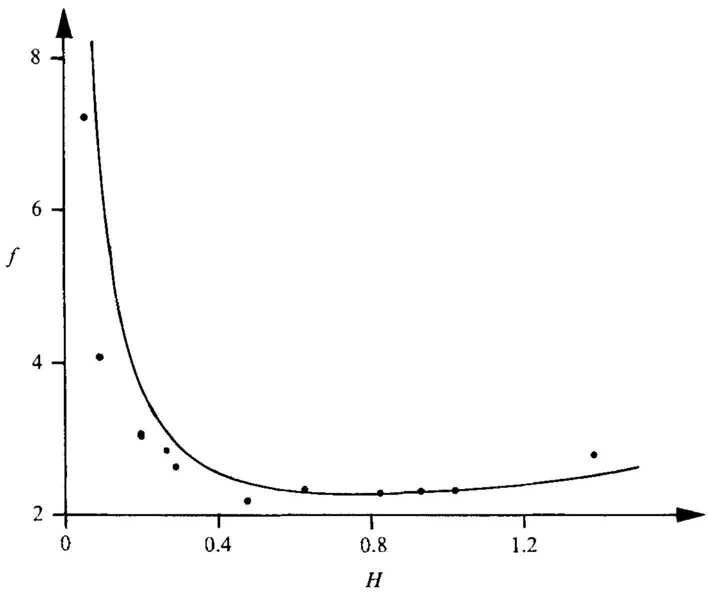

FIGURE 5. Measured critical values of f plotted against H, for silicone oil with viscosity 30770 cP.

figure 6. Although the experimental points with the three smallest values of H happen to be remarkably close to the theoretical curve, the overall comparison between theory and experiment is much less satisfactory than in figures 4 and 5. Experimental points in the range $0.4 < H < 0.9$ lie around 60% higher than the theoretical curve, which includes the minimum $f_c = 2.2$, approximately, at $H = 0.77$. The lack of agreement is attributable to the Weissenberg effects that were otherwise conspicuous in the experiments with the oil of highest viscosity. The observed

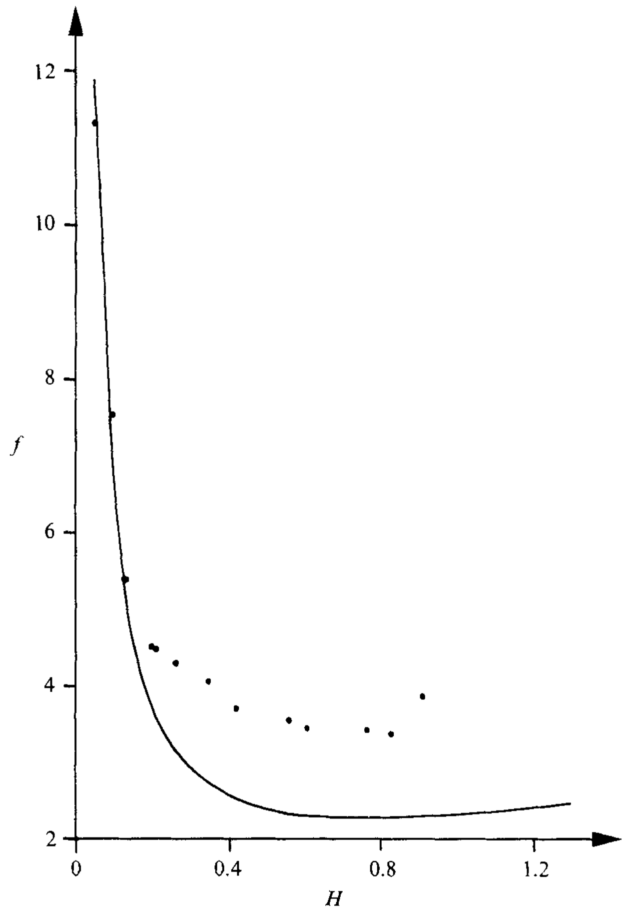

FIGURE 6. Measured critical values of f plotted against H, for silicone oil with viscosity 64000 cP.

thickening of the sheared layer at its inner edge, which implies thinning of the layer elsewhere, is a complication presumably sufficient to invalidate the present theoretical model. (Attempts by us to allow theoretically for non-Newtonian effects and so account better for the experimental results in figure 6 have been inconclusive, and we judge them to be not worth recording here.)

6. Discussion

It deserves emphasis that the measurements presented in figures 4–6 depended on a sensitive means of detecting the incipience of buckling. For the liquids with high viscosities yet free from significant non-Newtonian behaviour, a reasonably close agreement was thereby found between the observed thresholds of buckling and the predictions of the theory developed in §3. Our experience during the experiments showed, moreover, that distinctly higher values of f_c might well have been noted if we had relied on direct observation or on records of some gross property of the buckled layers.

The theoretical estimates (35) or (37) thus appear to be reliable predictions of the stability limit for a sheared layer, and the revealed dependence of f_c on H is the most interesting conclusion of the theory. When only marginally satisfied, however, the instability condition $f > f_c(H)$ does not imply that the layer will be prominently distorted by buckling; rather, the predicted waves will gradually become stronger as f is raised above $f_c(H)$. The experimental results at least confirm that the results of the new theory are more dependable than the estimate $f_c = 1/H$ given by the rudimentary theory reviewed in §2.

It remains to recognize that our experimental results differ substantially from those of Suleiman & Munson (1981), who used measurements of torque to detect buckling. On the basis of experiments using silicone oils with viscosities 9700, 29000 and 98000 cP and three different underlying liquids of comparatively negligible viscosity, they proposed $f > 4.1$ as a universal condition of buckling for thin layers. The critical value 4.1 estimated by them is almost twice the mean level of f_c in figures 4 and 5 over the range $0.3 < H < 0.8$, which appears to cover their experiments with water as the underlying liquid. Also, their experiments evidently missed the striking rise in f_c that both our theory and our experiments show to occur at smaller values of H. The importance of the non-dimensional form f for the shear stress was amply demonstrated by Suleiman & Munson's paper, but their measurements of critical values f_c seem to relate to a subsequent stage in the development of buckling, not to the onset of wave motion. Although there is some uncertainty about the actual values of the two surface tensions, it seems unlikely to account for the differences between their experimental results and ours: the same value of $T = T_1 + T_2$ was in fact used by them. Our experiments apparently realized comparative advantages from a much wider annular gap, which reduced complicating effects due to menisci, from a more sensitive means of detection and from a greater range of layer thicknesses.

We gratefully acknowledge the interdepartmental accord whereby facilities for our experiments were provided in the Clarendon Laboratory, Oxford. We are also indebted to the SERC for support and to Professor K. Walters, of the University College of Wales, Aberystwyth, for generous help in measuring properties of the silicone oils used in our experiments.

REFERENCES

BIOT, M. A. 1964 Theory of viscous buckling of multilayered fluids undergoing finite strain. *Phys. Fluids* **7**, 855–861.

BUCKMASTER, J. D. & NACHMAN, A. 1978 The buckling and stretching of a viscida. II. Effects of surface tension. *Q. J. Mech. Appl. Maths* **31**, 157–168.

DAVIES, J. T. & RIDEAL, E. K. 1961 *Interfacial Phenomena*. Academic.

LAMB, H. 1932 *Hydrodynamics*, 6th edn. Cambridge University Press. (Dover edition 1945.)

RAMBERG, H. 1963 Fluid dynamics of viscous buckling applicable to folding of layered rocks. *Bull. Am. Assoc. Petrol. Geol.* **47**, 484–505.

SULEIMAN, S. M. & MUNSON, B. R. 1981 Viscous buckling of thin fluid layers. *Phys. Fluids* **24**, 1–5.

TAYLOR, G. I. 1969 Instability of jets, threads and sheets of viscous fluid. *Proc. 12th Intl Cong. Appl. Mech., Stanford*, pp. 384–388. Springer.

TIMOSHENKO, S. 1940 *Theory of Plates and Shells*. McGraw-Hill.

WOLLKIND, D. J. & ALEXANDER, J. I. D. 1982 Kelvin–Helmholtz instability in a layered Newtonian fluid model of the geological phenomenon of rock folding. *SIAM J. Appl. Maths* **42**, 1276–1295.